Effect of anomalous elasticity on bubbles in van der Waals heterostructures

A. A. Lyublinskaya,[1,2] S. S. Babkin,[1,2] and I. S. Burmistrov[2,3]
[1]*Moscow Institute of Physics and Technology, 141700 Dolgoprudnyi, Moscow Region, Russia*
[2]*L. D. Landau Institute for Theoretical Physics, Semenova 1-a, 142432 Chernogolovka, Russia*
[3]*Laboratory for Condensed Matter Physics, National Research University Higher School of Economics, 101000 Moscow, Russia*

(Received 24 September 2019; accepted 4 March 2020; published 30 March 2020)

It is shown that the anomalous elasticity of membranes affects the profile and thermodynamics of a bubble in van der Waals heterostructures. Our theory generalizes the nonlinear plate theory as well as the membrane theory of the pressurised blister test to incorporate the power-law scale dependence of the bending rigidity and Young's modulus of a two-dimensional crystalline membrane. This scale dependence, caused by long-range interaction of relevant thermal fluctuations (flexural phonons), is responsible for the nonlinear Hooke law observed recently in graphene. It is shown that this anomalous elasticity affects the dependence of the maximal height of the bubble as a function of its radius and temperature. We determine the characteristic temperature above which the anomalous elasticity is important. It is suggested that, for graphene-based van der Waals heterostructures, the predicted anomalous regime is experimentally accessible at room temperature.

DOI: 10.1103/PhysRevE.101.033005

I. INTRODUCTION

Mechanical properties of two-dimensional (2D) materials, especially of the van der Waals (vdW) heterostructures, have recently attracted a great deal of interest in view of their potential applications [1]. The simplest example of the vdW heterostructure can be given by a bilayer formed from two monolayers of one atom thick, e.g., graphene, hexagonal boron nitride (hBN), and MoS_2, assembled together. The strong adhesion between monolayers [2] results in atomically clean interfaces in which all the contaminants aggregate in bubbles [3]. Recently, these bubbles inside the vdW heterostructures were studied experimentally [4]. Similar bubbles originate in the region between the atomic single layer and the substrate, e.g., SiO_2 [4,5]. There are many suggestions of practical usage of the bubbles inside the vdW heterostructures, for example, graphene liquid cell microscopy [6] and controlled room-temperature photoluminescence emitters [7].

The mechanics of monolayers due to these bubbles is considered to be analogous to that of the pressurized blister test, which has recently become the routine method to measure simultaneously Young's modulus and adhesion energy of a monolayer on a substrate [8–11]. Usually, the pressurized blister test is described either by the nonlinear plate model or by the membrane theory (see, e.g., [12,13]). These standard elastic theories of deformed plates ignore the fact that the elastic properties of an atomic monolayer are those of 2D crystalline membranes [14–20]. The striking feature of membrane mechanics is anomalous elasticity which results in the scale dependence of elastic moduli and in the nonlinear Hooke law for small tensile stress (see Refs. [21,22] for a review). These effects have been supported by atomistic calculations [23] and measured in graphene [24] (see also [25]).

Recently, the standard Föppl–von Kármán theory has been shown to be modified by anomalous elasticity for micron-size graphene samples at room temperature [26]. However, until recently (see, e.g., Refs. [27–30]), the anomalous elasticity has been completely ignored in the description of the mechanical and thermodynamic properties of bubbles inside vdW heterostructures.

In our paper we study the effect of anomalous elasticity on the mechanical and thermodynamic properties of bubbles inside vdW heterostructures. Our approach explicitly takes into account the power-law renormalization of elastic moduli. It is shown that above a certain temperature the dependence of the bending rigidity and Young's modulus of a membrane on the bubble radius results in the nonanalytic behavior of the maximum height of the bubble as a function of the radius and the temperature.

The outline of the paper is as follows. In Sec. II we formulate the model for description of elastic properties of the bubble between a membrane and a substrate. The standard approach to the problem is reviewed in Sec. III. The modifications of the standard approach due to the thermal fluctuations are studied in Sec. IV. In Sec. V we discuss how the power-law scaling of elastic moduli affects the thermodynamics of the bubbles. We conclude the paper with a discussion in Sec. VI and summary in Sec. VII. Some details are delegated to the Appendixes.

II. MODEL

The model for the description of the profile of a bubble between the membrane and the substrate (see Fig. 1) is well established [4,12]. It can be formulated in terms of the (free) energy, which is a sum of the following four terms:

$$E = E_{\rm bend} + E_{\rm el} + E_{\rm b} + E_{\rm vdW}. \tag{1}$$

The first term describes the energy cost related to the bending of the membrane

$$E_{\rm bend} = \frac{\varkappa_0}{2}\int d^2\boldsymbol{r}[(\Delta h)^2 + (\Delta \boldsymbol{u})^2], \tag{2}$$

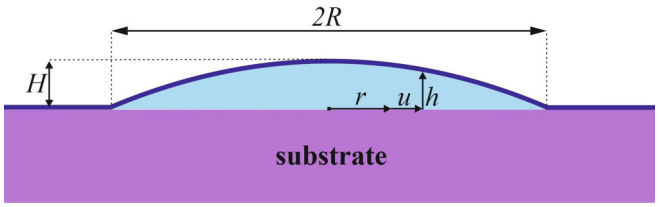

FIG. 1. Sketch of a spherical bubble enclosed within a membrane and a substrate.

where $\varkappa_0$ denotes the bare bending rigidity of the membrane. Here $\boldsymbol{u} = \{u_x, u_y\}$ and h are the in-plane and out-of-plane displacements of the membrane (see Fig. 1). The second term is the standard elastic energy [31]

$$E_{\rm el} = \int d^2\boldsymbol{r}(\mu_0 u_{\alpha\beta}u_{\beta\alpha} + \lambda_0 u_{\alpha\alpha}u_{\beta\beta}/2), \tag{3}$$

where μ_0 and λ_0 stand for the Lamé coefficients and $u_{\alpha\beta} = (\partial_\beta u_\alpha + \partial_\alpha u_\beta + \partial_\alpha h\partial_\beta h + \partial_\alpha \boldsymbol{u}\partial_\beta \boldsymbol{u})/2$ is the strain tensor. The third term $E_{\rm b}$ describes the contribution of the bubble substance. Under the assumption of a constant pressure P inside the bubble, one has $E_{\rm b} = -PV$, where the bubble volume can be approximated as $V = \int d^2\boldsymbol{r}\, h(\boldsymbol{r})$. The last term in Eq. (1) describes the vdW interaction between the membrane and the substrate in the presence of the bubble. It can be approximated as $E_{\rm vdW} = \pi\gamma R^2$. Here R denotes the radius of the bubble (see Fig. 1) and γ is the effective adhesion energy [4]. The form (1) of the total energy is well justified if the maximal height of the bubble $H = h(0)$ is small compared to the radius, $H \ll R$. We assume that this condition is fulfilled.

III. STANDARD APPROACH

In order to compute the profile of the spherical bubble, at first, one needs to solve the Euler-Lagrange equations for $\boldsymbol{u}(r)$ and $h(r)$ with the proper boundary conditions and compute the energy E as a function of R and H. Usually, instead of the solution of the Euler-Lagrange equations, the approximate solutions either within the nonlinear plate theory or within the membrane theory are used (see, e.g., Ref. [12]). Finally, one has to minimize E with respect to the both R and H. The minimization procedure allows one to find the maximal height H and the pressure P as a function of the bubble radius R. Comparison of the linear term in u and the term quadratic in h for the strain tensor $u_{\alpha\beta}$ leads to the following relation for the maximal horizontal deformation: $u_{\rm max} \sim H^2/R$. In the considered regime $H/R \ll 1$, the horizontal displacement is small as well, $u_{\rm max} \ll H$. This implies that one can neglect the term $\partial_\alpha \boldsymbol{u}\partial_\beta \boldsymbol{u}$ in $u_{\alpha\beta}$. Also this allows one to omit the term $(\Delta \boldsymbol{u})^2$ in the bending energy such that it reads

$$E_{\rm bend} = \frac{\varkappa_0}{2}\int d^2\boldsymbol{r}(\Delta h)^2. \tag{4}$$

In the absence of $\partial_\alpha \boldsymbol{u}\partial_\beta \boldsymbol{u}$ in $u_{\alpha\beta}$ the elastic energy becomes quadratic in $\boldsymbol{u}$. This implies that the Euler-Lagrange equation for $\boldsymbol{u}(\boldsymbol{r})$ becomes linear and can be solved for an arbitrary configuration of $h(\boldsymbol{r})$ (even not necessarily obeying the Euler-Lagrange equation). In other words, a horizontal deformation is matched to any vertical displacement. Therefore, $E_{\rm el}$ is given as [14]

$$E_{\rm el} = \frac{Y_0}{8}\int d^2\boldsymbol{r}\left(K_{\alpha\alpha} - \partial_\alpha \int d^2\boldsymbol{r}'\mathcal{G}(\boldsymbol{r},\boldsymbol{r}')\partial_\beta K_{\alpha\beta}(\boldsymbol{r}')\right)^2, \tag{5}$$

where $K_{\alpha\beta} = \partial_\alpha h\partial_\beta h$ and $Y_0 = \frac{4\mu_0(\mu_0+\lambda_0)}{2\mu_0+\lambda_0}$ is Young's modulus. The function $\mathcal{G}(\boldsymbol{r},\boldsymbol{r}')$ is the Green's function of the Laplace operator at the disk $r \leqslant R$.

Using Eqs. (4) and (5), we can estimate the bending and elastic energies as $E_{\rm bend} \sim \varkappa_0 H^2/R^2$ and $E_{\rm el} \sim Y_0 H^4/R^2$. For $H \gg a$, where $a \sim \sqrt{\varkappa_0/Y_0}$ is the effective thickness of the membrane, the elastic energy dominates over the bending energy, $E_{\rm el} \ll E_{\rm bend}$. We note that the effective thickness is typically smaller than the lattice spacing, e.g., for graphene $a \sim 1$ Å. Thus, by neglecting $E_{\rm bend}$ and minimizing $E_{\rm el} + E_{\rm b} + E_{\rm vdW}$ (with $E_{\rm b} \sim -PHR^2$) over H and R, we find

$$H = c_1 R(\gamma/Y_0)^{1/4}, \quad P = c_2(\gamma^3 Y_0)^{1/4}/R. \tag{6}$$

Here the coefficients $c_1 \approx 0.86$ and $c_2 \approx 1.84$ have been obtained from the approximate solution of the Euler-Lagrange equations for $h(r)$ and $\boldsymbol{u}(r)$ [12]. The results (6) are applicable under the conditions $\gamma \ll Y_0$ and $R \gg a(Y_0/\gamma)^{1/4}$, which guarantee $H \ll R$ and $H \gg a$, respectively. We note that the minimization of the energy implies $|E_{\rm b}| \sim E_{\rm vdW}$ entailing $P \sim \gamma/H$. This relation between P and H will hold for all regimes considered below. Therefore, in what follows we will present the expressions for the maximal height H alone.

IV. EFFECT OF THERMAL FLUCTUATIONS

The finite temperature induces thermal fluctuations of the membrane. These thermal fluctuations, in essence, originate from the in-plane and flexural (out-of-plane) phonons. The in-plane phonons induce the long-range interaction between flexural phonons [Eq. (5)]. The most hazardous phonons are the out-of-plane ones with the wave vectors $q < 1/R_*$ [14,15,18], where $R_* \sim \varkappa_0/\sqrt{Y_0 T}$ is the so-called Ginzburg length.[1] Therefore, at finite temperature for the bubble of radius $R > R_*$ one should integrate out the flexural phonons with momenta $1/R < q < 1/R_*$ before the derivation of the Euler-Lagrange equation for h. In essence, integration over the out-of-plane phonons leads to the same form of bending and elastic energies as given by Eqs. (4) and (5) but with a renormalized bending rigidity and Young's modulus [15]:

$$\varkappa(R) = \varkappa_0(R/R_*)^\eta, \quad Y(R) = Y_0(R/R_*)^{-2+2\eta}. \tag{7}$$

Here η is a universal exponent which depends on the dimensionality of a membrane and of an embedded space. For the clean 2D crystalline membrane in the three-dimensional space, the numerics predicts $\eta \approx 0.795 \pm 0.01$ [32].

The presence of nonzero tension σ affects the thermal fluctuations. There is a characteristic tension $\sigma_* = \varkappa_0/R_*^2 \sim TY_0/\varkappa_0$ [25,33–35]. For $\sigma \ll \sigma_*$, the scaling (7) holds for the interval $R_* \ll R \ll R_\sigma$, where $R_\sigma = R_*(\sigma/\sigma_*)^{1/(2-\eta)}$ is the solution of the equation $\sigma = \varkappa(R_\sigma)/R_\sigma^2$. For $R \gg R_\sigma$, the bending rigidity and Young's modulus saturate at the values

[1]The Ginzburg length corresponds to the size of a bubble of height a at which $E_{\rm bend} \sim T$.

$\varkappa(R_\sigma)$ and $Y(R_\sigma)$, respectively.[2] For $\sigma > \sigma_*$ ($R_\sigma < R_*$) the thermal fluctuations are completely suppressed and at finite temperature one can minimize the unrenormalized bending [Eq. (4)] and elastic [Eq. (5)] energies.

The pressure P inside the bubble results in nonzero tension $\sigma_P \sim PR_0$, where $R_0 \sim R^2/H$ is the radius of the curvature of the membrane on the bubble [36]. Using Eq. (6), we find $\sigma_P \sim \sqrt{\gamma Y_0}$. Such tension is sufficient to suppress the thermal fluctuations provided $\sigma_P \gg \sigma_*$, i.e., the standard approach is only valid at sufficiently low temperatures: $T \ll T_\gamma \sim \varkappa_0\sqrt{\gamma/Y_0}$. The energy scale T_γ has the clear physical meaning of the temperature at which the vdW energy for the bubble of radius R_* becomes of the order of the temperature. In other words, for $T \gg T_\gamma$ the vdW energy does not suppress the thermal fluctuations. Below we will study this regime.

A. Bending-dominated regime

We start from a bubble with the radius $R \ll R_*$. At such a small length scale there is no renormalization of the bending rigidity and Young's modulus. However, as follows from the above, the standard approach cannot be correct. The only resolution is the assumption that the bending energy dominates over elastic one, $E_{\rm bend} \gg E_{\rm el}$, i.e., $H \ll a$. After the minimization of $E_{\rm bend} + E_{\rm b} + E_{\rm vdW}$ over H and R, we find

$$H = c_3 a(T_\gamma/T)(R/R_*)^2, \quad R \ll R_*. \tag{8}$$

Here $c_3 \approx 0.65$ is found from the solution of the Euler-Lagrange equation for $h(r)$ (see Appendix A). For $T \gg T_\gamma$ the value of H for all $R \ll R_*$ is much smaller than a. This justifies the assumption of dominance of the bending energy for $R \ll R_*$.

Now we assume that the bubble radius is $R \gg R_*$. At such length scales one has to take into account the renormalization of the bending rigidity and Young's modulus (provided the scale R_σ is large enough). The renormalization changes the estimates for the bending and elastic energies: $E_{\rm bend} \sim \varkappa(R)H^2/R^2$ and $E_{\rm el} \sim Y(R)H^4/R^2$. Again we assume that the bending energy is larger than the elastic one, $E_{\rm bend} \gg E_{\rm el}$. This implies that $H \ll a(R/R_*)^{1-\eta/2}$. The minimization of $E_{\rm bend} + E_{\rm b} + E_{\rm vdW}$ yields

$$H = c_4 a(T_\gamma/T)(R/R_*)^{2-\eta/2}, \quad R_* \ll R \ll R_*T/T_\gamma, \tag{9}$$

where $c_4 \approx 0.90$ (see Appendix A). The dependence (9) is shown in Fig. 2.

The upper bound on R in Eq. (9) comes from the condition $E_{\rm bend} \gg E_{\rm el}$. In the above analysis we neglect the tension of the membrane due to the pressure. Using Eq. (9), we find the following estimate: $\sigma_P \sim \gamma(R/H)^2 \sim \sigma_*(R_*/R)^{2-\eta}$, i.e., $R_\sigma \sim R$. Since the power-law renormalization (7) is governed by the flexural phonons with momentum $q > 1/R$, the tension σ_P is indeed irrelevant for the thermal fluctuations in the regime $R_* \ll R \ll R_*T/T_\gamma$.

[2]Here we neglect the weak logarithmic dependence of the bending rigidity on R for $R \gg R_\sigma$ (cf. Ref. [34]). Such logarithmic corrections are beyond the accuracy of our estimates.

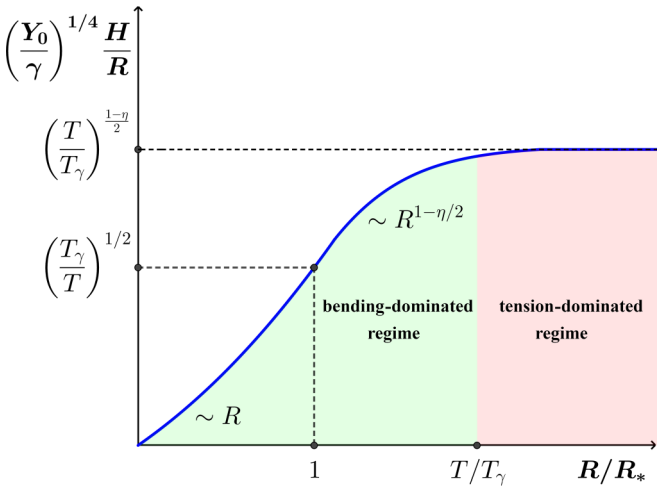

FIG. 2. Dependence of the aspect ratio on the radius of the bubble at high temperatures $T \gg T_\gamma$.

B. Tension-dominated regime

For the bubbles of radius $R \gg R_*T/T_\gamma$, the elastic energy dominates over the bending one, $E_{\rm el} \gg E_{\rm bend}$. Then the minimization of $E_{\rm el} + E_{\rm b} + E_{\rm vdW}$ over H and R implies that $E_{\rm el} \sim |E_{\rm b}| \sim E_{\rm vdW}$. Therefore, the pressure-induced tension is $\sigma_P \sim |E_{\rm b}|/H^2 \sim E_{\rm el}/H^2 \gg E_{\rm bend}/H^2$. This estimate means that the pressure-induced tension is important and the corresponding length scale is short, $R_\sigma \ll R$. In such a regime the bending rigidity and Young's modulus are independent of R, though strongly renormalized. Therefore, we can use the results of the standard approach but with Young's modulus $Y(R_\sigma)$ instead of Y_0. In particular, the tension induced by the pressure is given as $\sigma_P \sim \sqrt{\gamma Y(R_\sigma)}$. Hence the length scale R_σ satisfies the following equation: $\varkappa(R_\sigma)/R_\sigma^2 = \sqrt{\gamma Y(R_\sigma)}$. Its solution yields $R_\sigma \sim R_*T/T_\gamma$. This justifies that the profile of the bubbles with $R \gg R_*T/T_\gamma$ is governed by the pressure-induced tension. The characteristic radius R_σ has a simple physical meaning. The bubble of such a radius has the adhesion energy $\pi\gamma R_\sigma^2$ equal to T. Using Eq. (6) with the renormalized Young modulus, we find

$$H = c_1 a(R/R_*)(T/T_\gamma)^{-\eta/2}, \quad R_*T/T_\gamma \ll R. \tag{10}$$

We mention that although the aspect ratio H/R of the bubbles with $R \gg R_*T/T_\gamma$ is independent of R, it is not constant and depends on the temperature. The magnitude of the aspect ratio is much larger than one would predict on the basis of the standard approach. The behavior of the aspect ratio as a function of R at $T \gg T_\gamma$ is shown in Fig. 2.

V. ANOMALOUS THERMODYNAMICS

The temperature dependence of the maximal height H depends on the equation of state of the substance inside the bubble. We start from the case of a liquid bubble. Then we can approximate the equation of state for the liquid by the constant volume condition $V = \text{const}$. We start from the case of a bubble of sufficiently large volume $V \gg V_\gamma \sim a^3\varkappa_0/T_\gamma$.

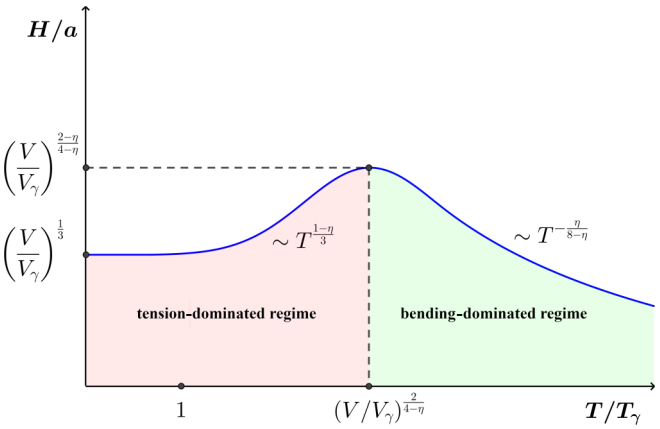

FIG. 3. Dependence of the maximal height of the liquid bubble versus temperature for the case of large volume $V \gg V_\gamma$.

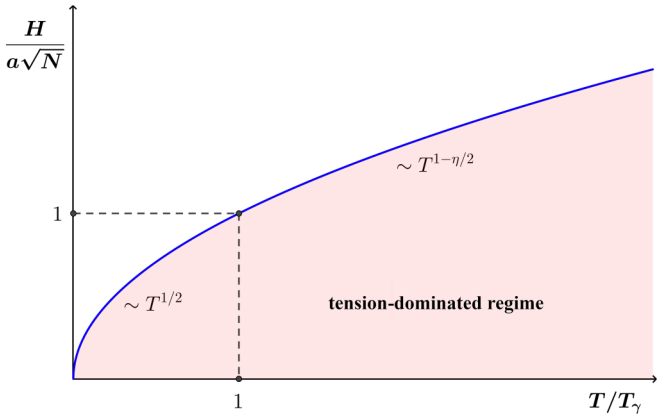

FIG. 4. Dependence of the maximal height of the bubble, with the ideal gas inside, on the temperature.

At low temperatures $T \ll T_\gamma$, the maximal height is given by Eq. (6), i.e., the height H is independent of T:

$$H \sim a(V/V_\gamma)^{1/3}, \quad T \ll T_\gamma. \tag{11}$$

At $T_\gamma \ll T \ll T_\gamma(V/V_\gamma)^{2/(4-\eta)}$ the thermal fluctuations are important but the physical behavior is governed with the pressure-induced tension. Using Eq. (10), we find

$$H \sim a\left(\frac{VT^{1-\eta}}{V_\gamma T_\gamma^{1-\eta}}\right)^{1/3}, \; T_\gamma \ll T \ll T_\gamma\left(\frac{V}{V_\gamma}\right)^{2/(4-\eta)}. \tag{12}$$

At high temperatures $T \gg T_\gamma(V/V_\gamma)^{2/(4-\eta)}$, the maximal height of the bubble is described by the theory of the bending-dominated regime [Eq. (9)]. Then we find that the height H decreases as the temperature increases:

$$H \sim a\left(\frac{V^{4-\eta}T_\gamma^{\eta}}{V_\gamma^{4-\eta}T^{\eta}}\right)^{1/(8-\eta)}, \quad T_\gamma\left(\frac{V}{V_\gamma}\right)^{2/(4-\eta)} \ll T. \tag{13}$$

Therefore, in the regime of large volumes $V \gg V_\gamma$, the maximal height of the bubble has a nonmonotonic dependence on the temperature with the maximum at temperature $T_{\max} \sim T_\gamma(V/V_\gamma)^{2/(4-\eta)}$ (see Fig. 3). The nonmonotonic dependence of H implies the change of the sign of the linear thermal expansion coefficient α_H at temperature $T_{\max}$:

$$\alpha_H = \frac{1}{T} \times \begin{cases} 0, & T \ll T_\gamma \\ \frac{1-\eta}{3}, & T_\gamma \ll T \ll T_{\max} \\ -\frac{\eta}{8-\eta}, & T_{\max} \ll T. \end{cases} \tag{14}$$

Therefore, by measuring the slope of α_H against $1/T$, one can extract the bending rigidity exponent of the membrane. The result (14) is derived with the neglect of the temperature dependence of the adhesion energy.

In the case of a bubble with a small volume of liquid $V \ll V_\gamma$, the temperature dependence of the maximal height is determined by the bending-dominated regime. At low temperatures, from Eq. (6) we obtain that the maximal height of the bubble is independent of temperature:

$$H \sim a(V/V_\gamma)^{1/2}, \quad T \ll T_\gamma(V/V_\gamma)^{-1/2}. \tag{15}$$

At high temperatures, as it follows from Eq. (10), the maximal height of the bubble starts to decrease with temperature:

$$H \sim a(V/V_\gamma)^{(4-\eta)/(8-\eta)}(T/T_\gamma)^{-\eta/(8-\eta)}, \quad T_\gamma(V/V_\gamma)^{-1/2} \ll T. \tag{16}$$

We note that the power-law decay is controlled by the bending rigidity exponent η. The decay of H with an increase of T implies the negative linear thermal expansion coefficient $\alpha_H = (1/H)dH/dT$. Although interesting on its own, the bubble with a liquid of small volume $V \ll V_\gamma$ can hardly be detected since, as it follows from Eqs. (15) and (16), the maximal height of the bubble is smaller than the effective thickness of the membrane a.

Now we discuss the case of a bubble with a gas inside. For the sake of simplicity, we use the equation of state of the ideal gas $PV = NT$, where N is the number of atoms of the gas. Using the relations $V \sim HR^2 \sim \gamma R^2/P$, we find that the radius of the bubble with the ideal gas is always given as $R \sim \sqrt{NT/\gamma}$. At low temperature $T \ll T_\gamma$, using Eq. (6), we find that the maximal height of the bubble grows with temperature as

$$H \sim a\sqrt{N}(T/T_\gamma)^{1/2}, \quad T \ll T_\gamma. \tag{17}$$

We note that, strictly speaking, this estimate is valid for $T \gg T_\gamma/N$. Under the assumption of a macroscopic number of atoms $N \gg 1$, inside the bubble this limitation on T is completely irrelevant.

For high temperatures $T \gg T_\gamma$, the bubbles of radius $R \gg R_* T/T_\gamma$ (this condition is equivalent to the condition $N \gg 1$) can only arise. Therefore, the bubble is in the tension-dominated regime when its maximal height is described by Eq. (10). Then we obtain

$$H \sim a\sqrt{N}(T/T_\gamma)^{1-\eta/2}, \quad T \gg T_\gamma. \tag{18}$$

The above results show that the maximal height of the bubble with the ideal gas inside is a monotonically growing function of temperature (see Fig. 4). Therefore, the linear thermal expansion coefficient is always positive:

$$\alpha_H = \frac{1}{T} \times \begin{cases} 1/2, & T \ll T_\gamma \\ 1 - \eta/2, & T_\gamma \ll T. \end{cases} \tag{19}$$

As in the case of a liquid bubble, the α_H versus T^{-1} slope allows one to extract the magnitude of η.

VI. DISCUSSION

Using a more realistic equation of state, one can compute the temperature dependence of the maximal height along the liquid-to-gas isotherm. In particular, one can analyze how the anomalous elasticity affects the liquid-to-gas transition in the bubble. This phenomenon was recently studied in Ref. [37] but within the standard approach, which ignores the thermal fluctuations of the membrane.

It is known [36,38] that the anomalous elasticity of a membrane affects the stability of the spherical membrane shells. The renormalization of the bending rigidity and Young's modulus decreases the pressure-induced tension towards the negative magnitudes sufficient for developing the buckling instability. In principle, a similar mechanism of instability is also applicable for the curved membrane above the bubble. However, our estimates indicate that such buckling instability is unattainable (see Appendix B).

Also, it is worthwhile to mention that in the bending-dominated regime there are large thermodynamical fluctuations of the bubble height which may complicate the experimental observation of the dependence predicted for the average height of the bubble on R and T (see Appendix C).

Let us estimate the relevant parameters for our theory in the case of the vdW heterostructure fabricated with the graphene monolayer on the hBN monolayer. Using the known magnitudes of Young's modulus, the bending rigidity, and the effective thickness of graphene, $Y_0 \approx 22\,\mathrm{eV\,\AA^{-2}}$, $\varkappa_0 \approx 1.1\,\mathrm{eV}$, and $a \approx 0.6\,\mathrm{\AA}$, respectively, we can estimate the Ginzburg length as $R_* \approx 4\,\mathrm{\AA}$ at $T = 300\,\mathrm{K}$ [33]. Assuming that the total adhesive energy is dominated by the adhesive energy between graphene and hBN, $\gamma \approx 0.008\,\mathrm{eV\,\AA^{-2}}$ [2], we find $T_\gamma \approx 250\,\mathrm{K}$. This estimate indicates that the aspect ratio of the bubbles between graphene and hBN measured recently [4] can be described by our theory in the tension-dominated regime [Eq. (10)]. Using the aspect ratio of 0.11 observed experimentally, we obtain $T_\gamma \approx 220\,\mathrm{K}$ and the adhesion energy $\gamma \approx 0.007\,\mathrm{eV\,\AA^{-2}}$. The latter is 20% larger than the magnitude extracted in Ref. [4] within the standard approach [Eq. (6)]. This implies that a proper account of the thermal fluctuations can be crucial for the precision measurements of the adhesion energy via the pressurized blister test. The characteristic volume for the bubble between graphene and hBN can be estimated as $V_\gamma \approx 10\,\mathrm{\AA^3}$. Such smallness of the magnitude of V_γ suggests that the nonmonotonic behavior of the maximal height of temperature in a graphene-on-hBN structure could only be observed experimentally for liquid bubbles with a radius of a few nanometers. We note that the temperature T_γ for the monolayer MoS_2 can be estimated to be larger than 1000 K due to large value of bending rigidity.

VII. SUMMARY

We have demonstrated that the anomalous elasticity of membranes affects the profile of a bubble in vdW heterostructures at high temperatures. We have extended the nonlinear plate theory as well as the membrane theory usually used for the description of the pressurized blister test to incorporate the power-law scale dependence of the bending rigidity and Young's modulus of a membrane. It was shown that the renormalization of the bending rigidity and Young's modulus results in the anomalous dependence of the maximal height of the bubble on its radius and temperature. We have predicted the nonmonotonic dependence of the maximal height of the liquid bubble inside the vdW heterostructure on the temperature. Our estimates suggest that for the graphene-based vdW heterostructures the anomalous regime predicted in the paper is experimentally accessible at ambient conditions.

ACKNOWLEDGMENTS

A.A.L. and S.S.B. are grateful to the FIZIKA foundation for support. I.S.B. is grateful to I. Gornyi, V. Kachorovskii, and A. Mirlin for very useful discussions as well as to I. Kolokolov and K. Tikhonov for valuable remarks. The work was partially supported by the programs of the Russian Ministry of Science and Higher Education, by the Russian Foundation for Basic Research (Grant No. 20-52-12019) Deutsche Forschungsgemeinschaft (Grant No. SCHM 1031/12-1) cooperation, and by the Basic Research Program of HSE.

APPENDIX A: MAXIMAL HEIGHT OF THE BUBBLE IN THE BENDING-DOMINATED REGIME

In this Appendix we present the accurate analytical calculation of the maximal height of the bubble in the bending-dominated regime.

Let us introduce the normalized eigenfunctions of the Laplace operator on the disk $r \leqslant R$ satisfying zero boundary conditions at $r = R$:

$$\Delta\phi_n(\boldsymbol{r}) = -\frac{\zeta_n^2}{R^2}\phi_n(\boldsymbol{r}),$$
$$\phi_n(\boldsymbol{r}) = \frac{1}{\sqrt{\pi}R|J_1(\zeta_n)|}J_0\left(\frac{\zeta_n r}{R}\right). \tag{A1}$$

Here ζ_n, with $n = 1, 2, \ldots$, are the zeros of the zeroth-order Bessel function $J_0(x)$. Then we can write the renormalized bending energy as

$$E_{\mathrm{bend}} = \frac{1}{2}\int d^2\boldsymbol{r}\, d^2\boldsymbol{r}'\, \Delta h(\boldsymbol{r})\hat{\varkappa}(\boldsymbol{r}-\boldsymbol{r}')\Delta h(\boldsymbol{r}'), \tag{A2}$$

where the integral operator $\hat{\varkappa}$ is defined via its action on the eigenfunctions of the Laplace operator:

$$\int d^2\boldsymbol{r}'\hat{\varkappa}(\boldsymbol{r}-\boldsymbol{r}')\phi_n(\boldsymbol{r}') = \zeta_n^{-\eta}\varkappa(R)\phi_n(\boldsymbol{r}). \tag{A3}$$

Here we recall that $\varkappa(R) = \varkappa_0(R/R_*)^\eta$.

Now let us expand the height of the bubble into the series: $h(\boldsymbol{r}) = \sum_n \alpha_n\phi_n(\boldsymbol{r})$. This expansion automatically satisfies the boundary condition $h(r = R) = 0$. The knowledge of the coefficients α_n allows one to find the maximal height of the bubble: $H = \sum_n \alpha_n/\sqrt{\pi}R|J_1(\zeta_n)|$. In terms of the coefficients α_n, the total energy acquires the following form:

$$E_{\mathrm{bend}} + E_{\mathrm{b}} + E_{\mathrm{vdW}} = \frac{\varkappa(R)}{2R^4}\sum_n \zeta_n^{4-\eta}\alpha_n^2 - 2\sqrt{\pi}PR\sum_n \frac{\mathrm{sgn}[J_1(\zeta_n)]}{\zeta_n}\alpha_n + \pi\gamma R^2. \tag{A4}$$

Its minimization over α_n yields

$$\alpha_n = 2\sqrt{\pi}\frac{PR^5}{\varkappa(R)}\frac{\mathrm{sgn}[J_1(\zeta_n)]}{\zeta_n^{5-\eta}}. \tag{A5}$$

Hence, for the total energy we obtain

$$E_{\mathrm{bend}} + E_{\mathrm{b}} + E_{\mathrm{vdW}} = -2\pi\frac{P^2R^6}{\varkappa(R)}\sum_n \zeta_n^{-6+\eta} + \pi\gamma R^2. \tag{A6}$$

Minimization with respect to R determines the pressure inside the bubble:

$$P = c_4'\frac{\sqrt{\gamma\varkappa(R)}}{R^2}, \quad c_4' = \left[(6-\eta)\sum_n \zeta_n^{\eta-6}\right]^{-1/2} \approx 9.72. \tag{A7}$$

Using this result for the pressure, we find the final expression for the maximal height:

$$H = 2\frac{PR^4}{\varkappa(R)}\sum_n \frac{\zeta_n^{-5+\eta}}{J_1(\zeta_n)} = c_4R^2\left(\frac{\gamma}{\varkappa(R)}\right)^{1/2},$$
$$c_4 = 2c_4'\sum_n \frac{\zeta_n^{-5+\eta}}{J_1(\zeta_n)} \approx 0.90. \tag{A8}$$

The constants c_3 and c_3' relevant for the low-temperature regime $R \ll R_*$ are obtained from the results above by setting $\eta = 0$. Then we find $c_3 \approx 0.65$ and $c_3' \approx 13.86$.

APPENDIX B: ABSENCE OF THE BUCKLING INSTABILITY OF A SPHERICAL BUBBLE

In this Appendix we demonstrate that there is no buckling transition of the bubble. In the presence of a nonzero curvature radius R_0 of the membrane, flexural phonons acquire a true mass equal to Y_0/R_0^2 [36]. This modification of the spectrum of flexural phonons results in negative renormalization of the tension. Perturbatively, a change of the tension $\delta\sigma$ can be estimated as [36]

$$\frac{\delta\sigma}{\sigma} \sim -\frac{TY_0^2}{\sigma R_0^2}\int \frac{d^2\boldsymbol{k}}{(2\pi)^2}\frac{k^2}{\left(\varkappa_0k^4 + \sigma k^2 + Y_0/R_0^2\right)^2}. \tag{B1}$$

We emphasize that here the integral over momentum k has infrared cutoff due to the radius of the bubble R: $k \gtrsim 1/R$.

Equation (B1) can be directly applied to the regime of low temperatures $T \ll T_\gamma$. Then, using Eq. (6), we find

$$\frac{\delta\sigma}{\sigma} \sim -\frac{T}{\gamma R^2}\ln\frac{R^2\sqrt{\gamma Y_0}}{\varkappa_0}. \tag{B2}$$

Since the low-temperature theory is applicable for $R \gg a(Y_0/\gamma)^{1/4}$, we find that $|\delta\sigma|/\sigma \ll (T/T_\gamma)^2 \ll 1$.

Now let us consider the regime of high temperatures $T \gg T_\gamma$. For $R \ll R_*$ we can use Eq. (B1). Then, using Eq. (9), we obtain ($x = kR$)

$$\frac{\delta\sigma}{\sigma} \sim -\left(\frac{T_\gamma}{T}\right)^2\left(\frac{R}{R_*}\right)^6\int_{\sim 1} dx\frac{x^3}{\left(x^4 + x^2 + \gamma Y_0R^4/\varkappa_0^2\right)^2}. \tag{B3}$$

Since the parameter $\gamma Y_0R^4/\varkappa_0^2)^2 \sim (T_\gamma/T)^2(R/R_*)^4 \ll 1$, integrating over x, we find

$$\frac{\delta\sigma}{\sigma} \sim -\left(\frac{T_\gamma}{T}\right)^2\left(\frac{R}{R_*}\right)^6. \tag{B4}$$

Therefore, we find that $|\delta\sigma|/\sigma \ll (T_\gamma/T)^2 \ll 1$ for $R \ll R_*$. In the case of an intermediate radius $R_* \ll R \ll R_\sigma = R_*T/T_\gamma$, we need to modify Eq. (B1) in order to include renormalization of the bending rigidity and Young's modulus:

$$\frac{\delta\sigma}{\sigma} \sim -\frac{TY(R)^2}{\sigma R_0^2}\int \frac{d^2\boldsymbol{k}}{(2\pi)^2}\frac{k^2}{[\varkappa(R)k^4 + \sigma k^2 + Y(R)/R_0^2]^2}. \tag{B5}$$

Using Eq. (10), we obtain

$$\frac{\delta\sigma}{\sigma} \sim -\left(\frac{R}{R_\sigma}\right)^2\int_{\sim 1} dx\frac{x^3}{[x^4 + x^2 + \gamma Y(R)R^4/\varkappa^2(R)]^2}. \tag{B6}$$

Since $\gamma Y(R)R^4/\varkappa^2(R) \sim (R/R_\sigma)^2 \ll 1$, we obtain

$$\frac{|\delta\sigma|}{\sigma} \sim \left(\frac{R}{R_\sigma}\right)^2 \ll 1, \quad R_* \ll R \ll R_\sigma. \tag{B7}$$

Finally, we consider the case $R \gg R_\sigma$. Here we can use Eq. (B2) with $\varkappa_0$ and Y_0 replaced by $\varkappa(R_\sigma)$ and $Y(R_\sigma)$, respectively. Then we find

$$\frac{|\delta\sigma|}{\sigma} \sim \left(\frac{R_\sigma}{R}\right)^2\ln\frac{R}{R_\sigma} \ll 1, \quad R \gg R_\sigma. \tag{B8}$$

The above results demonstrates that for both low- and high-temperature regimes, the renormalization of the tension due to the finite curvature is weak and cannot lead to the buckling instability. The only exception is the bubbles with the radius $R \sim R_\sigma$ for which our estimates give $|\delta\sigma|/\sigma \sim 1$. This implies that for $R \sim R_\sigma$ the buckling instability could occur in principle. In order to resolve this issue one needs to perform a more accurate renormalization-group scheme similar to the one of Ref. [38]. However, since for $R \ll R_\sigma$ and $R \gg R_\sigma$ the buckling instability is absent, the scenario with instability for $R \sim R_\sigma$ seems to be unlikely.

APPENDIX C: THERMODYNAMIC FLUCTUATIONS OF THE HEIGHT OF THE BUBBLE

In this Appendix we estimate the thermodynamic fluctuations of the height of the bubble in the bending-dominated regime $R \ll R_*T/T_\gamma$. Using Eq. (4), we find

$$\langle(\delta H)^2\rangle \sim T\int \frac{d^2\boldsymbol{k}}{(2\pi)^2}\frac{1}{\varkappa(R)k^4}. \tag{C1}$$

As above, the integral over momentum k has infrared cutoff due to the radius of the bubble R: $k \gtrsim 1/R$. Hence we find that the dispersion of height fluctuations is given as

$$\langle(\delta H)^2\rangle \sim TR^2/\varkappa(R). \tag{C2}$$

Then for $R \ll R_*T/T_\gamma$ we obtain the following estimate:

$$\frac{\sqrt{\langle(\delta H)^2\rangle}}{H} \sim \frac{T}{T_\gamma}\frac{R_*}{R} \gg 1. \tag{C3}$$

This inequality implies that there are large thermodynamic fluctuations of the height of the bubble in the bending-dominated regime.

For the tension-dominated regime $R \gg R_\sigma = R_* T/T_\gamma$ we need to take into account the tension induced by the pressure:

$$\langle (\delta H)^2 \rangle \sim T \int \frac{d^2\boldsymbol{k}}{(2\pi)^2} \frac{1}{\varkappa(R_\sigma)k^4 + \sigma_P k^2} \sim \frac{T R_\sigma^2}{\varkappa(R_\sigma)} \ln \frac{R}{R_\sigma}. \tag{C4}$$

Then we obtain the following estimate:

$$\frac{\sqrt{\langle (\delta H)^2 \rangle}}{H} \sim \frac{T}{T_\gamma} \frac{R_*}{R} \ln \frac{R}{R_\sigma} \ll 1. \tag{C5}$$

Therefore, the thermodynamic fluctuations of the height of the bubble in the tension-dominated regime are strongly suppressed.

[1] Z. Dai, L. Liu, and Z. Zhang, Strain engineering of 2D materials: Issues and opportunities at the interface, Adv. Mater. **31**, 1805417 (2019).

[2] Y. T. Megra and J. W. Suk, Adhesion properties of 2D materials, J. Phys. D **52**, 364002 (2019).

[3] S. J. Haigh, A. Gholinia, R. Jalil, S. Romani, L. Britnell, D. C. Elias, K. S. Novoselov, L. A. Ponomarenko, A. K. Geim, and R. Gorbachev, Cross-sectional imaging of individual layers and buried interfaces of graphene-based heterostructures and superlattices, Nat. Mater. **11**, 764 (2012).

[4] E. Khestanova, F. Guinea, L. Fumagalli, A. K. Geim, and I. V. Grigorieva, Universal shape and pressure inside bubbles appearing in van der Waals heterostructures, Nat. Commun. **7**, 12587 (2016).

[5] Z. Dai, Y. Hou, D. A. Sanchez, G. Wang, C. J. Brennan, Z. Zhang, L. Liu, and N. Lu, Interface-Governed Deformation of Nanobubbles and Nanotents Formed by Two-Dimensional Materials, Phys. Rev. Lett. **121**, 266101 (2018).

[6] S. M. Ghodsi, C. M. Megaridis, R. Shahbazian-Yassar, and T. Shokuhfar, Advances in graphene-based liquid cell electron microscopy: Working principles, opportunities, and challenges, Small Methods **3**, 1900026 (2019).

[7] A. V. Tyurnina, D. A. Bandurin, E. Khestanova, V. G.Kravets, M. Koperski, F. Guinea, A. N. Grigorenko, A. K. Geim, and I. V. Grigorieva, Strained bubbles in van der Waals heterostructures as local emitters of photoluminescence with adjustable wavelength, ACS Photon. **6**, 516 (2019).

[8] S. P. Koenig, N. G. Boddeti, M. L. Dunn, and J. S. Bunch, Ultrastrong adhesion of graphene membranes, Nat. Nanotechnol. **6**, 543 (2011).

[9] N. G. Boddeti, X. Liu, R. Long, J. Xiao, J. S. Bunch, and M. L. Dunn, Graphene blisters with switchable shapes controlled by pressure and adhesion, Nano Lett. **13**, 6216 (2013).

[10] D. Lloyd, X. Liu, N. Boddeti, L. Cantley, R. Long, M. L. Dunn, and J. S. Bunch, Adhesion, stiffness, and instability in atomically thin MoS_2 bubbles, Nano Lett. **17**, 5329 (2017).

[11] G. Wang, Z. Dai, J. Xiao, S. Feng, C. Weng, L. Liu, Z. Xu, R. Huang, and Z. Zhang, Bending of Multilayer van der Waals Materials, Phys. Rev. Lett. **123**, 116101 (2019).

[12] K. Yue, W. Gao, R. Huang, and K. M. Liechti, Analytical methods for the mechanics of graphene bubbles, J. Appl. Phys. **112**, 083512 (2012).

[13] P. Wang, W. Gao, Z. Cao, K. M. Liechti, and R. Huang, Numerical analysis of circular graphene bubbles, J. Appl. Mech. **80**, 040905 (2013).

[14] D. R. Nelson and L. Peliti, Fluctuations in membranes with crystalline and hexatic order, J. Phys. (Paris) **48**, 1085 (1987).

[15] J. A. Aronovitz and T. C. Lubensky, Fluctuations of Solid Membranes, Phys. Rev. Lett. **60**, 2634 (1988).

[16] M. Paczuski, M. Kardar, and D. R. Nelson, Landau Theory of the Crumpling Transition, Phys. Rev. Lett. **60**, 2638 (1988).

[17] F. David and E. Guitter, Crumpling transition in elastic membranes: Renormalization group treatment, Europhys. Lett. **5**, 709 (1988).

[18] J. Aronovitz, L. Golubovic, and T. C. Lubensky, Fluctuations and lower critical dimensions of crystalline membranes, J. Phys. (Paris) **50**, 609 (1989).

[19] E. Guitter, F. David, S. Leibler, and L. Peliti, Thermodynamical behavior of polymerized membranes, J. Phys. (Paris) **50**, 1787 (1989).

[20] P. Le Doussal and L. Radzihovsky, Self-Consistent Theory of Polymerized Membranes, Phys. Rev. Lett. **69**, 1209 (1992).

[21] *Statistical Mechanics of Membranes and Surfaces*, edited by D. Nelson, T. Piran, and S. Weinberg (World Scientific, Singapore, 1989).

[22] P. Le Doussal and L. Radzihovsky, Anomalous elasticity, fluctuations and disorder in elastic membranes, Ann. Phys. (NY) **392**, 340 (2018).

[23] J. H. Los, A. Fasolino, and M. I. Katsnelson, Scaling Behavior and Strain Dependence of In-Plane Elastic Properties of Graphene, Phys. Rev. Lett. **116**, 015901 (2016).

[24] R. J. T. Nicholl, H. J. Conley, N. V. Lavrik, I. Vlassiouk, Y. S. Puzyrev, V. P. Sreenivas, S. T. Pantelides, and K. I. Bolotin, The effect of intrinsic crumpling on the mechanics of free-standing graphene, Nat. Commun. **6**, 9789 (2015).

[25] I. V. Gornyi, V. Y. Kachorovskii, and A. D. Mirlin, Anomalous Hooke's law in disordered graphene, 2D Mater. **4**, 011003 (2016).

[26] J. H. Los, A. Fasolino, and M. I. Katsnelson, Mechanics of thermally fluctuating membranes, npj 2D Mater. Appl. **1**, 9 (2017).

[27] H. Ghorbanfekr-Kalashami, K. S. Vasu, R. R. Nair, François M. Peeters, and M. Neek-Amal, Dependence of the shape of graphene nanobubbles on trapped substance, Nat. Commun. **8**, 15844 (2017).

[28] K. Zhang and M. Arroyo, Coexistence of wrinkles and blisters in supported graphene, Extreme Mech. Lett. **14**, 23 (2017).

[29] M. R. Delfani, Nonlinear elasticity of monolayer hexagonal crystals: Theory and application to circular bulge test, Eur. J. Mech. A **68**, 117 (2018).

[30] D. A. Sanchez, Z. Dai, P. Wang, A. Cantu-Chavez, C. J. Brennan, R. Huang, and N. Lu, Mechanics of spontaneously formed nanoblisters trapped by transferred 2D crystals, Proc. Natl. Acad. Sci. USA **115**, 7884 (2018).

[31] L. D. Landau and E. M. Lifshitz, *Theory of Elasticity* (Butterworth-Heinemann, Oxford, 2012).

[32] A. Tröster, Fourier Monte Carlo simulation of crystalline membranes in the flat phase, J. Phys.: Conf. Ser. **454**, 012032 (2013).

[33] R. Roldán, A. Fasolino, K. V. Zakharchenko, and M. I. Katsnelson, Suppression of anharmonicities in crystalline membranes by external strain, Phys. Rev. B **83**, 174104 (2011).

[34] A. Košmrlj and D. R. Nelson, Response of thermalized ribbons to pulling and bending, Phys. Rev. B **93**, 125431 (2016).

[35] I. S. Burmistrov, I. V. Gornyi, V. Y. Kachorovskii, M. I. Katsnelson, and A. D. Mirlin, Quantum elasticity of graphene: Thermal expansion coefficient and specific heat, Phys. Rev. B **94**, 195430 (2016).

[36] J. Paulose, G. A. Vliegenthart, G. Gompper, and D. R. Nelson, Fluctuating shells under pressure, Proc. Natl. Acad. Sci. USA **109**, 19551 (2012).

[37] P. Zhilyaev, E. Iakovlev, and I. Akhatov, Liquid–gas phase transition of ar inside graphene nanobubbles on the graphite substrate, Nanotechnology **30**, 215701 (2019).

[38] A. Košmrlj and D. R. Nelson, Statistical Mechanics of Thin Spherical Shells, Phys. Rev. X **7**, 011002 (2017).